Published in final edited form as:
Vis Neurosci. 2005 ; 22(4): 383–393. doi:10.1017/S095252380522401X.

Wide-field ganglion cells in macaque retinas

ELIZABETH S. YAMADA[1,2], **ANDREA S. BORDT**[1], and **DAVID W. MARSHAK**[1]
[1]Department of Neurobiology and Anatomy, University of Texas Medical School, Houston
[2]Departamento de Fisiologia, Universidade Federal do Pará, Belém, Brasil

Abstract

To describe the wide-field ganglion cells, they were injected intracellularly with Neurobiotin using an *in vitro* preparation of macaque retina and labeled with streptavidin-Cy3. The retinas were then labeled with antibodies to choline acetyltransferase and other markers to indicate the depth of the dendrites within the inner plexiform layer (IPL) and analyzed by confocal microscopy. There were eight different subtypes of narrowly unistratified cells that ramified in each of the 5 strata, S1–5, including narrow thorny, large sparse, large moderate, large dense, large radiate, narrow wavy, large very sparse, and fine very sparse. There were four types of broadly stratified cells with dendritic trees extending from S4 to S2. One type resembled the parvocellular giant cell and another the broad thorny type described previously in primates. Another broadly stratified cell was called multi-tufted based on its distinctive dendritic branching pattern. The fourth type had been described previously, but not named; we called it broad wavy. There was a bistratified type with its major arbor in S5, the same level as the blue cone bipolar cell; it resembled the large, bistratified cell with blue ON-yellow OFF responses described recently. Two wide-field ganglion cell types were classified as diffuse because they had dendrites throughout the IPL. One had many small branches and was named thorny diffuse. The second was named smooth diffuse because it had straighter dendrites that lacked these processes. Dendrites of the large moderate and multi-tufted cells cofasciculated with ON-starburst cell dendrites and were, therefore, candidates to be ON- and ON–OFF direction-selective ganglion cells, respectively. We concluded that there are at least 15 morphoplogical types of wide-field ganglion cells in macaque retinas.

Keywords

Acetylcholine; Plexiform; Stratification; Confocal

Introduction

In primates, the three most common types of retinal ganglion cells are midget, parasol, and small bistratified, and together these comprise approximately 75% of the ganglion cells in peripheral macaque retina (Dacey, 1994). The remaining retinal ganglion cells are quite heterogeneous, but they have larger dendritic arbors and are, therefore, called wide-field cells (Peterson & Dacey, 1999, 2000). Wide-field ganglion cells have been described in primate retinas stained using the Golgi method (Polyak, 1941; Rodieck, 1988; Kolb et al., 1992), and retrograde labeling studies indicate that various types of wide-field cells project to the lateral geniculate nucleus, the superior colliculus, or the pretectum (Rodieck & Watanabe, 1993; Dacey et al., 2003). In extracellular recordings from the central macaque

Address correspondence and reprint requests to: David W. Marshak, Department of Neurobiology and Anatomy, University of Texas Medical School, PO Box 20708, Houston, TX 77225, USA. david.w.marshak@uth.tmc.edu.

retina, some wide-field cells have phasic responses to both the onset and the offset of light stimuli; others have more sustained light responses (Schiller & Malpeli, 1977). A third type is unresponsive to stationary stimuli but inhibited by motion (de Monasterio, 1978). These and other wide-field ganglion cells would probably have been encountered more frequently in the peripheral retina. For example, a large, bistratified type of ganglion cell with blue ON-yellow OFF responses was recently identified in the peripheral macaque retina (Dacey et al., 2003).

The number of distinct types of wide-field ganglion cells is still unknown, however. One reason why it has been difficult to classify these cells morphologically is uncertainty about the depths of their dendritic arbors in the inner plexiform layer (IPL), a parameter that is critically important in determining the polarity and kinetics of their light responses (Roska & Werblin, 2001; Rockhill et al., 2002). Therefore, we injected wide-field ganglion cells intracellularly with Neurobiotin and then estimated the depth of their dendritic arbors using antibodies that label single, narrow strata in the IPL. Antibody against choline acetyltransferase (ChAT) was used in all retinas, and the other antibody was against either calbindin or tyrosine hydroxylase. Based on this information, we have identified 15 types of wide-field ganglion cells, including several that have been described previously in other mammals.

As Rodieck and Brening (1983) pointed out more than 20 years ago, this is only the beginning of a long process to demonstrate that these groupings, indeed, represent distinct types of ganglion cells and to establish their homology with similar types in other mammalian retinas. A much larger sample of labeled cells would be required to quantitatively describe the morphology of their perikarya, axons, and dendrites and to determine how these parameters vary with eccentricity. It is also essential to correlate morphology of each type of ganglion cell with its light responses, but this has been accomplished only once for wide-field cells in primates, with the large bistratified cells (Dacey et al., 2003).

Materials and methods

Macaque eyes were obtained within 10 min after the animal had been euthanized with an overdose of sodium pentobarbital (50–100 mg/kg I.V.) at the conclusion of experiments not related to our study. Animal protocols were approved by the University of Texas Health Science Center Animal Care and Use Committee. The eyes were kept in glass jars packed in ice for approximately 15 min and were then hemisected using a razor blade. The eyecups were immersed in oxygenated Ames medium (Sigma, St. Louis, MO), and the vitreous humor was removed with fine forceps. The procedure for intracellular injection was the same as described previously (Jacoby et al., 2000). Briefly, pieces of retina were stained with a 10 μM solution of acridine orange in Ames medium for 4 min. Then the tissue was mounted with the ganglion cell layer up in a chamber on an upright, fixed-stage microscope, and continuously superfused with oxygenated Ames medium at 20°C. Microeletrodes were made from thin-walled borosilicate glass using a P-87 micropipette puller (Sutter Instruments, Novato, CA). The tip resistance was between 50 and 100 MΩ. Microelectrodes were filled with a solution containing 2.5% Lucifer Yellow (Molecular Probes, Eugene, OR) and 5% Neurobiotin (Vector Laboratories, Burlingame, CA) in 20 mM 3-[N-morpholino] propanesulfonic acid (MOPS; Sigma) at pH 7.6. Ganglion cell somas were injected first with Lucifer Yellow using negative current pulses (2 Hz, 5–10 nA) until the dendrites began to fill, and then Neurobiotin was injected by switching the polarity of the injecting current to positive for 3–6 min. After several cells had been successfully injected, the tissue was fixed overnight in 2% paraformaldehyde in 0.1 M phosphate buffer (PB), pH 7.4. The injected

cells were all located in the peripheral retina near the horizontal meridian, and either the fovea or the optic disk was used to determine eccentricity.

Neurobiotin was visualized by incubating the tissue for 1–2 days in 1:200 streptavidin conjugated to indocarbocyanine (Cy3; Jackson Immunoresearch Laboratories, West Grove, PA) in 0.1 M phosphate-buffered saline (PBS), pH 7.4, with 0.3% Triton X-100. The tissue was then incubated for 5–10 days in primary antibodies diluted in PBS with 0.1% sodium azide and 0.3% Triton X-100. The primary antibodies and dilution used were affinity purified goat anti-choline acetyltransferase 1:200 (Chemicon International, Inc., Temecula, CA) and either monoclonal antibody to the calcium-binding protein calbindin D-28k 1:1000 (Sigma), or mouse anti-tyrosine hydroxylase 1:10,000 (Sigma). Secondary antibodies made in donkey were conjugated to either fluorescein isothiocyanate (FITC) or indodicarbocyanine (Cy5; Jackson). The pieces of retina were rinsed several times in PBS and mounted in glycerol with paraphenyline diamine.

Images were acquired using a confocal microscope (Zeiss LSM410, Thornwood, NY) with a krypton-argon laser, a 20× dry objective and also 40× and 63× oil-immersion objectives. Excitation was at 488 for FITC, 568 nm for Cy3, and 647 nm for Cy5. Emission filters were 515–540 nm for FITC, 590–610 nm for Cy3, and 670–810 nm for Cy5. Typically, 30–50 0.5-μm-thick optical sections were obtained. Five wide-field ganglion cells were analyzed further using a Zeiss LSM 510 Meta confocal laser scanning microscope with Argon/2, HeNe1 and HeNe2 lasers, and a 63× oil-immersion objective at high zoom. Excitation was 488 for Lucifer Yellow, 543 for Cy3, and 633 for Cy5. Emission filters were BP 505–530 for Lucifer Yellow, BP 560–613 for Cy3, and 657.4–743 nm in the META channel for Cy5. All images had a *z*-interval of 0.5 μm. Images were analyzed using Amira v.3.2 (TGS, San Diego, CA) to determine pixel intensity per slice and the data for each channel were graphed using Microsoft Excel (Microsoft Corporation, Redmond, WA).

To produce the figures, these digital images were processed in Adobe Photoshop (Adobe Systems, San Jose, CA) to enhance the color and contrast. This software was also used to count branch points in the unistratified cells, as described previously by Peterson and Dacey (1999). Ganglion cell densities were estimated using the method described previously by Wässle and Riemann (1978). For one cell, a cofasciculation index was calculated as described previously by Dong et al. (2004). Three optical sections from different regions of the dendritic tree having extensive interactions between ganglion cell dendrites and ChAT-immunoreactive (IR) processes were selected for analysis. The Histogram function of the LSM 510-Expert Mode was used to find values for the number of pixels in each channel and the number of pixels labeled in both channels, and the calculations were done using Excel. To estimate the number of contacts expected by chance, the channel with the ChAT label was rotated 90 deg, and the analysis was repeated.

Results and discussion

We selected small- to medium-sized perikarya under visual control, and labeled cells were identified as ganglion cells by the presence of an axon. This procedure yielded many types of wide-field ganglion cells, but it is possible that types with larger perikarya were undersampled. For comparison, we also injected parasol and midget ganglion cells in the same pieces of retina (Fig. 1A). In most cases, the difference in dendritic-field sizes between the wide-field cells and the largest parasol cells were large enough to leave no doubt that they were different. In the few cases when the differences in dendritic-field sizes were smaller, the dendritic morphology and branching patterns were quite different.

The first classification we made was based on the depth of dendritic stratification in the IPL. The depth was assigned based on the relationship between the dendrites of the injected

ganglion cell and the processes of retinal cells labeled with antibodies. Dopaminergic cells stratify in S1 (reviewed by Marshak, 2001). Dendrites of OFF-starburst amacrine cells and axon terminals of DB3 bipolar cells overlap in S2, and the dendrites of ON-starburst cells ramify in S4 (Rodieck & Marshak, 1992; Jacoby et al., 2000). Cells that had dendrites between the starburst bands were assigned to S3, and cells with dendrites below the ON-starburst band were assigned to S5. Examples of this depth analysis are shown in Figs. 1B–1F. According to the depth of dendritic stratification, macaque wide-field ganglion cells were classified into four groups: narrowly unistratified, broadly stratified, bistratified, and diffuse.

The narrowly unistratified cells had their entire dendritic trees in one stratum of the IPL; we found examples ramifying in each stratum. We identified eight different types of cells in this group and named them according to their dendritic morphology and branch densities. In Figs. 2 and 4, we show an example of each type in comparison to midget, parasol, and small bistratified cells (Figs. 2A–2C).

The narrow thorny (Figs. 2D–2E) cells had tortuous and fine dendrites with many branchlets and spine-like processes, as described previously (Dacey et al., 2003), and they resembled G8 and G16 cells in human retina (Kolb et al., 1992). Each subtype branched in a distinct stratum of the IPL. Some cells had dendrites in S5, and the remaining narrow thorny cells stratified in the center of the IPL, S3. In macaques, the narrow thorny cells project to the lateral geniculate nucleus (LGN) (Dacey et al., 2003). The narrow thorny cells of macaques resembled G1 cells of rabbit retina (Rockhill et al., 2002), G5 and G9 types of ground squirrel retinas (Linberg et al., 1996), and C4 cells of mouse retinas (Sun et al., 2002). The narrow thorny cells ramifying in S3 also resembled the zeta cells in cat retinas (Berson et al., 1998) and local edge detectors in rabbit (Amthor et al., 1989) retinas.

There were three additional types that resembled narrowly unistratified ganglion cells in human retinas. Previously, these had been divided into groups, rather than types, based on dendritic branch density (Peterson & Dacey, 1999). The cells we called large sparse had a regular branching pattern with relatively thin dendrites in S4; they were tracer coupled to amacrine cells (Fig. 2F). These cells had, on average, 56 branch points (± 8.5 S.D.), a value placing them in the large sparse group. Our large sparse cells resembled one of the cells of this group illustrated by Peterson and Dacey (1999; their Fig. 11) and type G20 of Kolb et al. (1992). Large sparse cells are known to project to the LGN in macaques (Dacey et al., 2003).

There was another cell ramifying in S4 with a denser arbor (Fig. 2G), which we called large moderate because it had 71 branch points (Peterson & Dacey, 1999); it also resembled type G21 of Kolb et al. (1992). The large moderate cell cofasciculated with starburst amacrine cells and received numerous contacts (Fig. 3A). The average cofasciculation index was 10.9, as opposed to 1.0 in controls (Dong et al., 2004). In this respect, it was similar to the ON direction-selective cells of rabbits (Famiglietti, 1992*b*). Many of the ganglion cells projecting to the nucleus of the optic tract are morphologically similar to our large moderate cell (Pu & Amthor, 1990), and it also resembled one of the ON direction-selective cells identified by intracellular recording and dye injection (He & Masland, 1998; their Fig. 2C).

Another type of narrowly stratified ganglion cell that we called large dense had a space-filling dendritic arbor in S2 (Fig. 2H). This cell had 142 branch points, a value placing it in the large dense group (Peterson & Dacey, 1999). The large dense cell also resembled the maze cells that project to the superior colliculus in macaques (Rodieck & Watanabe, 1993).

The most common of all wide-field ganglion cells in our sample ($n = 9$) had thick dendrites with a radiate, small-angle branching pattern, little overlap between neighboring dendrites

and a thick axon; we called these large radiate cells (Fig. 4A). There were two subtypes of large radiate cells stratifying in either S2 or S4. On average, these had 83 branch points (± 8.7 S.D.) in their dendritic trees, a value that places them in the moderately dense group. However, in humans, ganglion cells like this were classified as large sparse using the same criterion (Peterson & Dacey, 1999, Fig. 7A); this discrepancy is probably attributable to the larger sizes of the cells in humans. Large radiate cells are very similar to cat alpha cells (Boycott & Wässle, 1974), which have brisk transient responses to light (Cleland et al., 1975). The large radiate cells also resembled class I and G11 cells of rabbit retina (Rockhill et al., 2002; Famiglietti, 2004). It is possible that large radiate cells project to the magnocellular layers of the LGN. Some cells there have nonlinear spatial summation within their receptive-field centers, like cat alpha cells (Enroth-Cugell & Robson, 1966). Nonlinear magnocellular cells also have lower spatial resolution than the more common type (Kaplan & Shapley, 1982), as would be expected if they received input from ganglion cells with larger dendritic fields than parasol cells.

We also found narrowly unistratified cells in the macaque retina that resembled other well-characterized types of cat retinal ganglion cells, including delta, epsilon, and gamma. One that we called narrow wavy based on its dendritic morphology (Fig. 4B) had very tortuous dendrites in S1 of the IPL, like G19 cells of the human retinas (Kolb et al., 1992) and cat delta cells. In some instances, cells with a similar morphology branched in S2, instead (not illustrated). In the cat retina, delta cells accumulate monoamines (Wässle et al., 1987; Dacey, 1989). A morphologically similar type, G7, has been described in ground squirrel retina (Linberg et al., 1996).

One cell had very large and very sparse dendritic tree in S4, and we named it large very sparse accordingly (Fig. 4C). The large very sparse cell in our sample had a 786-μm-diameter dendritic field and 21 branching points, values placing it halfway between the large very sparse and giant very sparse groups in human retina (Peterson & Dacey, 1999). Both giant very sparse and large very sparse cells occur as ON and OFF subtypes in humans, and they are also coupled to amacrine cells (Peterson & Dacey, 1999). The large very sparse cell also resembled the macaque PT-sparse cells that project to the pretectum in macaques (Rodieck & Watanabe 1993), human G20 cells (Kolb et al., 1992), and cat epsilon cells. In cats, epsilon cells have sustained, ON-center responses with concentric OFF surrounds, and they project to the geniculate wing (Pu et al., 1994).

One cell type in our sample had a very small perikaryon and very fine dendrites with almost no branching (3 branch points); we named it fine very sparse (Fig. 4D). This cell stratified in S5, but otherwise, it resembled G3 cells described previously in humans (Kolb et al., 1992). Ganglion cells like these have been filled in the macaque retina after retrograde labeling from the pretectum; these cells occur as both inner and outer subtypes and have very sparse branching (Dacey et al., 2003; their Fig. 7C). The fine very sparse cell also resembled gamma cells from macaques (Rodieck & Watanabe, 1993) and cats (Boycott & Wässle, 1974).

We classified four types of cells as broadly stratified because their dendritic trees spanned the three contiguous strata in the middle of the IPL. The first of these, broad thorny cells, had dendrites very similar in morphology to the narrow thorny cells, and without depth markers, they might have been classified incorrectly (Fig. 5A). Indeed, Polyak (1941) seems to have classified all three types as garland cells. However, the dendrites of the broad thorny cells extended from S2 to S4, and they resembled G5 cells of human retinas (Kolb et al., 1992). These cells have been described previously in macaques and are known to project to the LGN (Dacey et al., 2003). However, broad thorny cells also resembled some T-group cells of macaques that project to the superior colliculus (Rodieck & Watanabe, 1993), and

therefore, they might project to both targets. Broad thorny cells resemble theta cells of cat retina (Isayama et al., 2000). However, both the T-group cells and cat theta cells are described as bistratified, whereas there were no obvious gaps in the dendritic arbors of broad thorny cells. In the cat retina, theta cells have phasic ON–OFF responses and axons with slow conduction velocities (Isayama et al., 2000).

We also observed one broadly stratified cell branching throughout the middle third of the IPL whose branches were more dense in the peripheral part of the dendritic field than in the central part (Fig. 5B). Based on this unusual dendritic branching pattern, we named it multi-tufted (Famiglietti, 1992*a*). In these respects, it resembled the ganglion cells with relatively dense dendritic arbors projecting to the pretectum in macaques (Rodieck & Watanabe, 1993; their Fig. 4) and the iota cell of the cat retina (O'Brien et al., 2002). The innermost dendrites cofasciculated with those of ON-cholinergic amacrine cells and received many contacts (Fig. 3B). Taken together, these findings suggest that, like iota cells of cat retinas (Isayama et al., 2000), multi-tufted cells are homologues of ON–OFF direction-selective ganglion cells in rabbits.

Another type of broadly stratified ganglion cell was named broad wavy because its dendrites were smooth and curved, overlapping extensively. These cells were tracer coupled to at least two other types of cells (Fig. 5C). Broad wavy cells resembled cells that project to the superior colliculus (Rodieck & Watanabe, 1993; their Fig. 6, center). In human retinas, a very similar cell was described as bistratified (Peterson & Dacey; their Fig. 4B) or as G23 (Kolb et al., 1992). A similar cell was described, but not classified, in the rabbit retina (Rockhill et al., 2002; their Fig. 3B).

The last type of broadly stratified ganglion cell (Fig. 5D) resembled the parvocellular giant cell described previously (Rodieck, 1988; Rodieck & Watanabe, 1993). These authors proposed that parvocellular giant cells project to the interlaminar zones associated with the parvocellular layers of the LGN. In human retinas, a member of the large moderate group is very similar to the parvo-cellular giant cell (Peterson & Dacey, 1999; their Fig. 7B).

The second most common cells in our sample ($n = 8$) were large bistratifed cells (Fig. 6). They were clearly distinguishable from the small bistratifed cells based on their much larger dendritic-field sizes (Fig. 1). The inner dendrites ramified in S4 and S5 and formed complete, robust trees, and the outer trees were made up of a few branches that originated from the inner trees and ascended to branch in S2. The large bistratified cells also showed heterologous coupling with wide-field amacrine cells. They resembled the large bistratified cells (Peterson & Dacey, 2000) and G17 cells (Kolb et al., 1992) in human retinas. In macaques, large bistratified cells like these have blue ON-yellow OFF responses to light and project to the LGN (Dacey et al., 2003).

We classified wide-field ganglion cells that branched in all strata of the IPL as diffuse, as in other recent studies (Kolb et al., 1992; Peterson & Dacey, 2000). Two cell types fell into this category. We named the first diffuse thorny because the dendrites had many small projections similar to those on the narrow and broad thorny cells (Fig. 7A). In this respect, they were similar to garland cells (Polyak, 1941). They also resembled the G4 cells (Kolb et al., 1992) and densely branched diffuse cells (Peterson & Dacey, 2000) in human retinas.

We named the other type smooth diffuse because its dendrites lacked these specializations. Smooth diffuse cells were tracer coupled to amacrine cells with perikarya in the inner nuclear layer (Fig. 7B) and resembled G22 cells of the human retina (Kolb et al., 1992).

To ensure that we had not overestimated the number of wide-field ganglion cell types, we calculated the density of each type based on the dendritic-field sizes 8–12 mm from the

fovea and a constant coverage factor of 3 (Dacey, 1994; Wässle & Riemann, 1978). Considering only the cell types described in this study, the total density of wide-field ganglion cells at this eccentricity would be 339/mm^2, but the total density of wide-field ganglion cells is approximately 600/mm^2 at this eccentricity (Dacey, 1994). One indication there are more than 15 types of wide-field ganglion cells is that several types of wide-field ganglion cells described by Kolb et al. (1992) in the human retina were not included in our sample. Another is that we did not inject any of the melanopsin containing ganglion cells described recently (Peterson et al., 2003).

In summary, we have described 15 morphological types of wide-field ganglion cells in the macaque retina (Fig. 8). We began with the classification scheme proposed most recently, the groups of wide-field ganglion cells described by Peterson and Dacey (1999, 2000). Using markers to indicate depth in the IPL, we subdivided these groups into distinct types, and whenever possible, we used names that were identical or quite similar to theirs. In Table 1, we also indicate how these ganglion cells have been classified in previous studies of primate retinas. Based on the cofasciculation with starburst cell dendrites, we identified two types of wide-field cells that resembled direction-selective ganglion cells in rabbits (Famiglietti, 1992*b*). Because three types of wide-field ganglion cells had subtypes branching in two different strata, there may be as many as 18 physiological types. One type of wide-field ganglion cell, the large bistratified cell, has been studied by intracellular recording and tracer injection in macaques (Dacey et al., 2003). The light responses of large radiate cells were predicted from extracellular recordings in the LGN of macaques (Kaplan & Shapley, 1982). Otherwise, the predictions regarding the light responses were based on studies in other mammals, and the light responses of these cells will need to be investigated in primates.

Acknowledgments

This work was supported by grants EY06472 and EY10608 from the National Eye Institute. E.S. Yamada was a recipient of CNPq fellowship No. 350117/99-3, a Latin American Scholars fellowship from the Pew Charitable Trusts and PRONEX-FINEP grant No. 76.97.1028.00. We are grateful to Dr. Roger Price of the M.D. Anderson Cancer Center for providing the tissue used in these studies, to Mr. Lorenzo Morales for drawing Fig. 8 and to Mrs. Lillemor Krosby for expert technical assistance. We also wish to thank Drs. Dennis Dacey, Edward Famiglietti, Helga Kolb, and Richard Masland for valuable discussions.

References

Amthor FR, Takahashi ES, Oyster CW. Morphologies of rabbit retinal ganglion cells with complex receptive fields. Journal of Comparative Neurology. 1989; 280:97–121. [PubMed: 2918098]

Berson DM, Pu M, Famiglietti EV. The zeta cell: A new ganglion cell type in cat retina. Journal of Comparative Neurology. 1998; 399:269–288. [PubMed: 9721908]

Boycott BB, Wässle H. The morphological types of ganglion cells of the domestic cat's retina. Journal of Physiology. 1974; 240:397–419. [PubMed: 4422168]

Cleland BG, Levick WR, Wässle H. Physiological identification of a morphological class of cat retinal ganglion cells. Journal of Physiology. 1975; 248:151–171. [PubMed: 1151804]

Dacey DM. Monoamine-accumulating ganglion cell type of the cat's retina. Journal of Comparative Neurology. 1989; 288:59–80. [PubMed: 2794138]

Dacey DM. Physiology, morphology and spatial densities of identified ganglion cell types in primate retina. Ciba Foundation Symposium. 1994; 184:12–28. discussion 28–34, 63–70. [PubMed: 7882750]

Dacey DM, Peterson BB, Robinson FR, Gamlin PD. Fireworks in the primate retina: In vitro photodynamics reveals diverse LGN-projecting ganglion cell types. Neuron. 2003; 37:15–27. [PubMed: 12526769]

de Monasterio FM. Properties of ganglion cells with atypical receptive-field organization in retina of macaques. Journal of Neuro-physiology. 1978; 41:1435–1449.

Dong W, Sun W, Zhang Y, Chen X, He S. Dendritic relationship between starburst amacrine cells and direction selective ganglion cells in the rabbit retina. Journal of Physiology 556. 2004; 1:11–17.

Enroth-Cugell C, Robson JG. The contrast sensitivity of retinal ganglion cells of the cat. Journal of Physiology. 1966; 187:517–552. [PubMed: 16783910]

Famiglietti EV. New metrics for analysis of dendritic branching patterns demonstrating similarities and differences in ON and ON–OFF directionally selective retinal ganglion cells. Journal of Comparative Neurology. 1992a; 324:295–321. [PubMed: 1383290]

Famiglietti EV. Dendritic co-stratification of ON and ON–OFF directionally selective ganglion cells with starburst amacrine cells in rabbit retina. Journal of Comparative Neurology. 1992b; 324:322–335. [PubMed: 1383291]

Famiglietti EV. Class I and class II ganglion cells of rabbit retina: A structural basis for X and Y (brisk) cells. Journal of Comparative Neurology. 2004; 478:323–346. [PubMed: 15384072]

He S, Masland RH. ON direction-selective ganglion cells in the rabbit retina: Dendritic morphology and pattern of fasciculation. Visual Neuroscience. 1998; 15:369–375. [PubMed: 9605536]

Isayama T, Berson DM, Pu M. Theta ganglion cell type of cat retina. Journal of Comparative Neurology. 2000; 417:32–48. [PubMed: 10660886]

Jacoby RA, Wiechmann AF, Amara SG, Leighton BH, Marshak DW. Diffuse bipolar cells provide input to OFF parasol ganglion cells in the macaque retina. Journal of Comparative Neurology. 2000; 416:6–18. [PubMed: 10578099]

Kaplan E, Shapley RM. X and Y cells in the lateral geniculate nucleus of macaque monkeys. Journal of Physiology. 1982; 330:125–143. [PubMed: 7175738]

Kolb H, Linberg KA, Fisher SK. Neurons of the human retina: A Golgi study. Journal of Comparative Neurology. 1992; 318:147–187. [PubMed: 1374766]

Linberg KA, Suemune S, Fisher SK. Retinal neurons of the California ground squirrel, Spermophilus beecheyi: A Golgi study. Journal of Comparative Neurology. 1996; 365:173–216. [PubMed: 8822165]

Marshak DW. Synaptic inputs to dopaminergic neurons in mammalian retinas. Progress in Brain Research. 2001; 131:83–91. [PubMed: 11420984]

O'Brien BJ, Isayama T, Richardson R, Berson DM. Intrinsic physiological properties of cat retinal ganglion cells. Journal of Physiology. 2002; 538:787–802. [PubMed: 11826165]

Peterson BB, Dacey DM. Morphology of wide-field, mono-stratified ganglion cells of the human retina. Visual Neuroscience. 1999; 16:107–120. [PubMed: 10022482]

Peterson BB, Dacey DM. Morphology of wide-field bistratified and diffuse human retinal ganglion cells. Visual Neuroscience. 2000; 17:567–578. [PubMed: 11016576]

Peterson BB, Liao H-W, Dacey DM, Yau K-W, Gamlin PD, Robinson FR, Marshak DW. Functional architecture of the photoreceptive ganglion cell in primate retina: Morphology, mosaic organization and central targets of melanopsin immunostained cells. Investigative Ophthalmology and Visual Science. 2003; 44:2003. program no 5182.

Polyak, SL. The Retina. University of Chicago Press; Chicago, Illinois: 1941.

Pu ML, Amthor FR. Dendritic morphologies of retinal ganglion cells projecting to the nucleus of the optic tract in the rabbit. Journal of Comparative Neurology. 1990; 302:657–674. [PubMed: 1702123]

Pu M, Berson DM, Pan T. Structure and function of retinal ganglion cells innervating the cat's geniculate wing: An *in vitro* study. Journal of Neuroscience. 1994; 14:4338–4358. [PubMed: 8027783]

Rockhill RL, Daly FJ, MacNeil MA, Brown SP, Masland RH. The diversity of ganglion cells in a mammalian retina. Journal of Neuroscience. 2002; 22:3831–3843. [PubMed: 11978858]

Rodieck, RW. The primate retina.. In: Steklis, HD., editor. Comparative Primate Biology. Alan R. Liss, Inc.; New York: 1988. p. 203-278.

Rodieck RW, Brening RK. Retinal ganglion cells: Properties, types, genera, pathways and trans-species comparisons. Brain, Behavior, and Evolution. 1983; 23:121–164.

Rodieck RW, Marshak DW. Spatial density and distribution of choline acetyltransferase immunoreactive cells in human, macaque and baboon retinas. Journal of Comparative Neurology. 1992; 321:46–64. [PubMed: 1613139]

Rodieck RW, Watanabe M. Survey of the morphology of macaque retinal ganglion cells that project to the pretectum, superior colliculus, and parvicellular laminae of the lateral geniculate nucleus. Journal of Comparative Neurology. 1993; 338:289–303. [PubMed: 8308173]

Roska B, Werblin F. Vertical interactions across ten parallel, stacked representations in the mammalian retina. Nature. 2001; 410:583–587. [PubMed: 11279496]

Schiller PH, Malpeli JG. Properties and tectal projections of monkey retinal ganglion cells. Journal of Neurophysiology. 1977; 40:428–445. [PubMed: 403252]

Sun W, Li N, He S. Large-scale morphological survey of mouse retinal ganglion cells. Journal of Comparative Neurology. 2002; 451:115–126. [PubMed: 12209831]

Wässle H, Voigt T, Patel B. Morphological and immunocytochemical identification of indoleamine-accumulating neurons in the cat retina. Journal of Neuroscience. 1987; 7:1574–1585. [PubMed: 3553450]

Wässle H, Riemann HJ. The mosaic of nerve cells in the mammalian retina. Proceedings of the Royal Society B (London). 1978; 200:441–461.

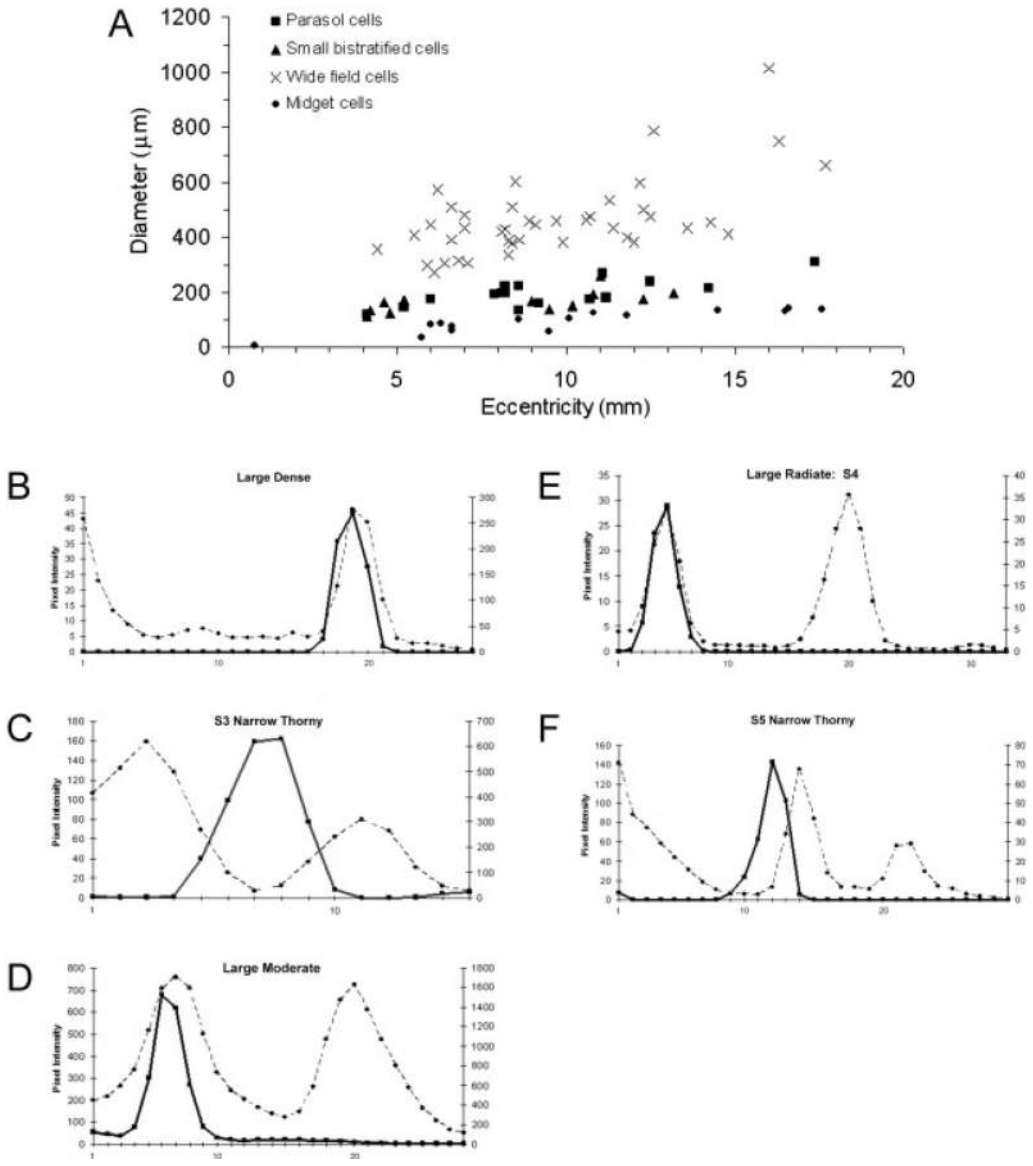

Fig. 1.

A: Dendritic-field size *vs.* eccentricity for the cells in our sample. Filled gray squares are parasol cells, open triangles are small bistratified cells, open circles are wide-field ganglion cells, and black diamonds are midget cells. There was no overlap between the wide field cells and any other group. B–F. Graphs of pixel intensity in thousands per optical section. The left side of the graph is closest to the ganglion cell layer and the right side is closest to the inner nuclear layer. Wide-field ganglion cell dendrites are represented by a heavy solid line and ChAT-IR processes by a dashed line. Two peaks of ChAT label demarcate S2 and S4. B: Large Dense cell, S2. C: Narrow Thorny cell, S3. D: Large Moderate cell, S4. E: Large Radiate ganglion cell, S4. F: Narrow Thorny ganglion cell, S5.

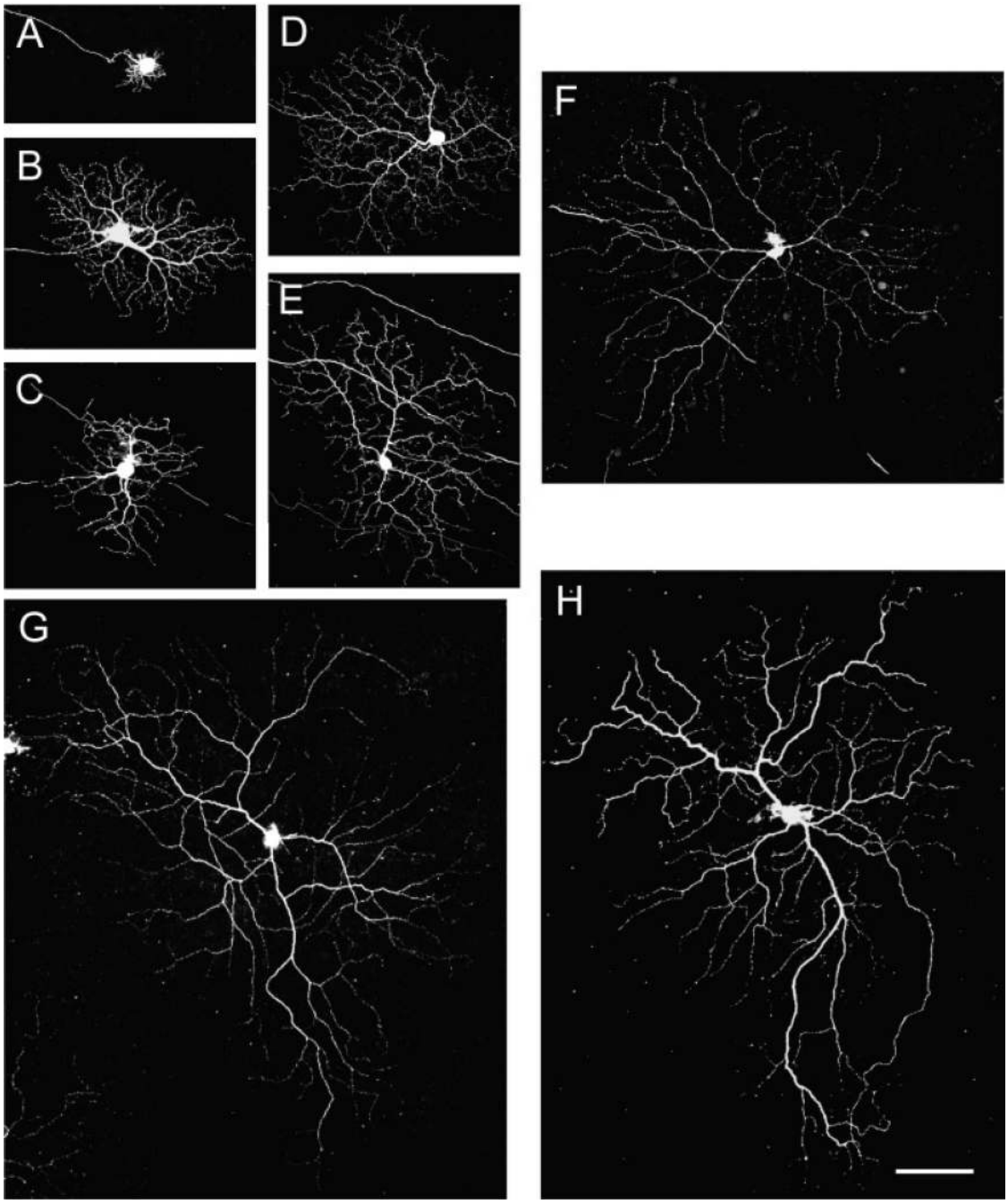

Fig. 2.

A midget, a parasol, and a small bistratified ganglion cell are shown in A–C with four different types of narrowly stratified wide-field ganglion cells of macaque retina (D–H). A: Inner midget cell at 9.5 mm nasal. B: Inner parasol cell at 8.2 mm temporal. C: Small bistratified cell at 10.8 mm nasal. D: S3 narrow thorny cell at 7.1 mm temporal. E: S5 narrow thorny cell at 6.8 mm nasal. F: Large sparse cell at 10.7 mm nasal. G: Large moderate cell at 8.5 mm nasal. H: Large dense cell at 12.2 mm nasal. Scale bar = 100 μm.

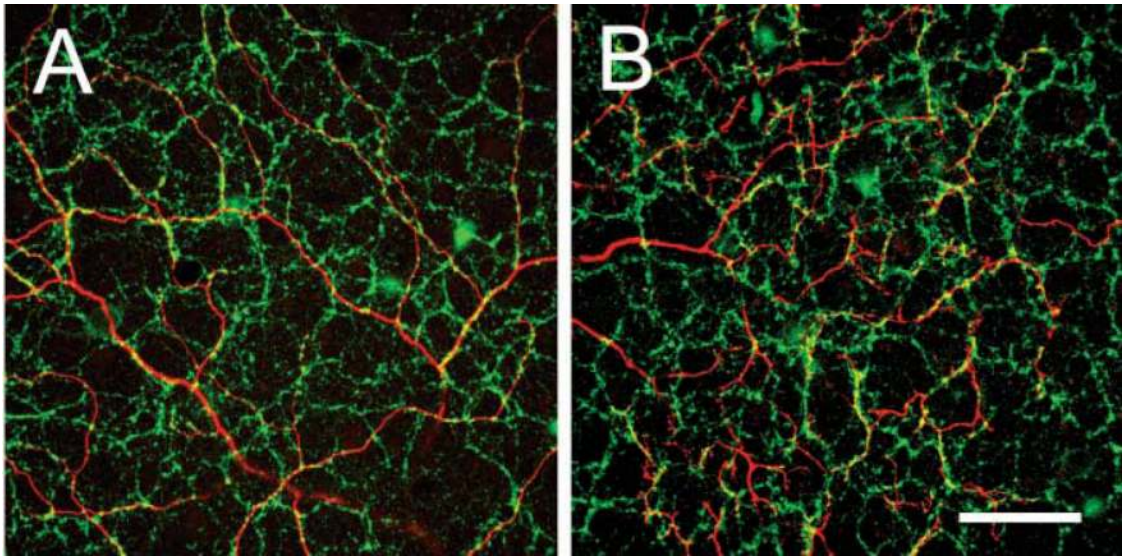

Fig. 3.

Cofasciculation of the dendrites of wide-field ganglion cells (RED) and ON-starburst amacrine cells (GREEN). A: Dendrites of the large moderate cell illustrated in Fig. 2G. This cell was narrowly stratified in S4 and received many contacts from ON-starburst dendrites. B: Another cell type, the multi-tufted cell, was broadly stratified. It also received numerous contacts from ON-starburst dendrites. In both cases, the number of yellow pixels was over three times higher in the original image in comparison to images in which the red and green channels rotated by 90 deg, 180 deg, and 270 deg. Scale bar = 50 μm.

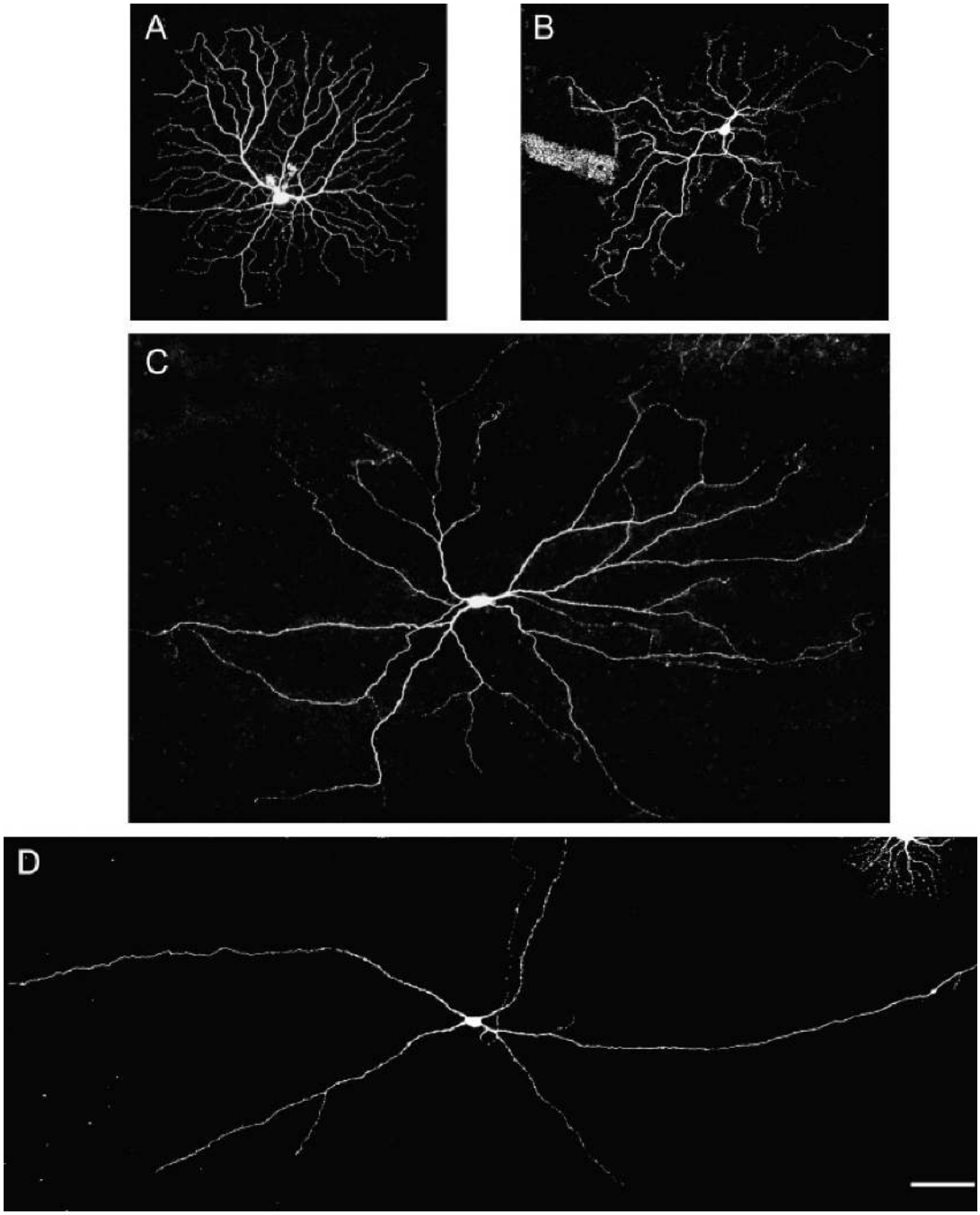

Fig. 4.

Wide-field ganglion cells in macaque retina that resemble narrowly unistratified cell types of the cat retina. A: Inner large radiate cell at 9.1 mm nasal. B: S1 narrow wavy cell at 6 mm temporal. C: Large very sparse cell at 12.6 mm nasal. D: Fine very sparse cell at 16 mm. Scale bar = 100 μm.

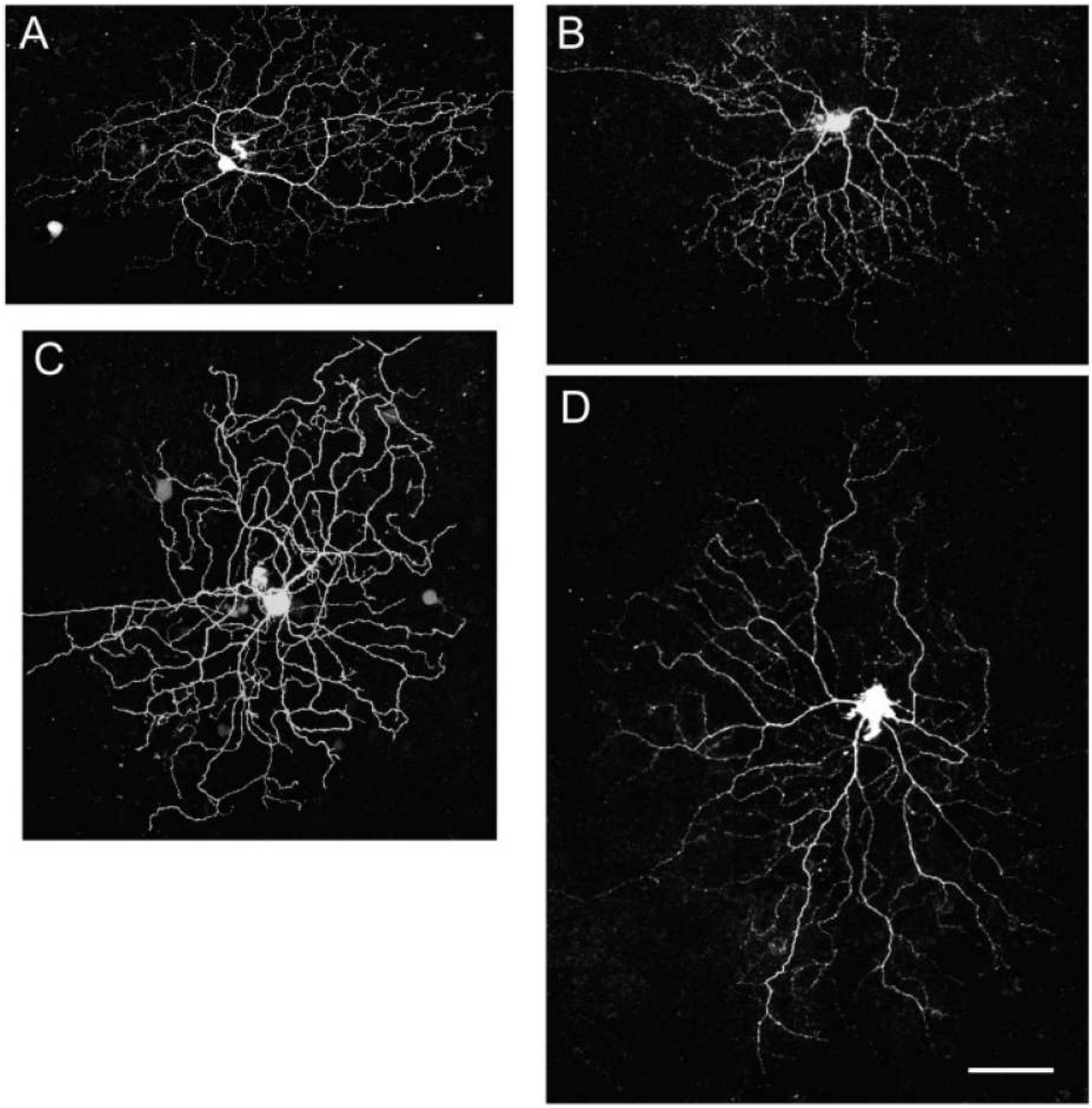

Fig. 5.

Four types of wide-field ganglion cells in macaque retina with broad stratification. All four types had dendrites occupying strata from S2 to S4. A: Broad thorny cell 14.8 mm nasal. B: Multi-tufted cell 8.6 mm nasal (also illustrated in 3B). C: Broad wavy cell 8.4 mm nasal. D: Parvocellular giant cell 16.3 mm temporal. Scale bar = 100 μm.

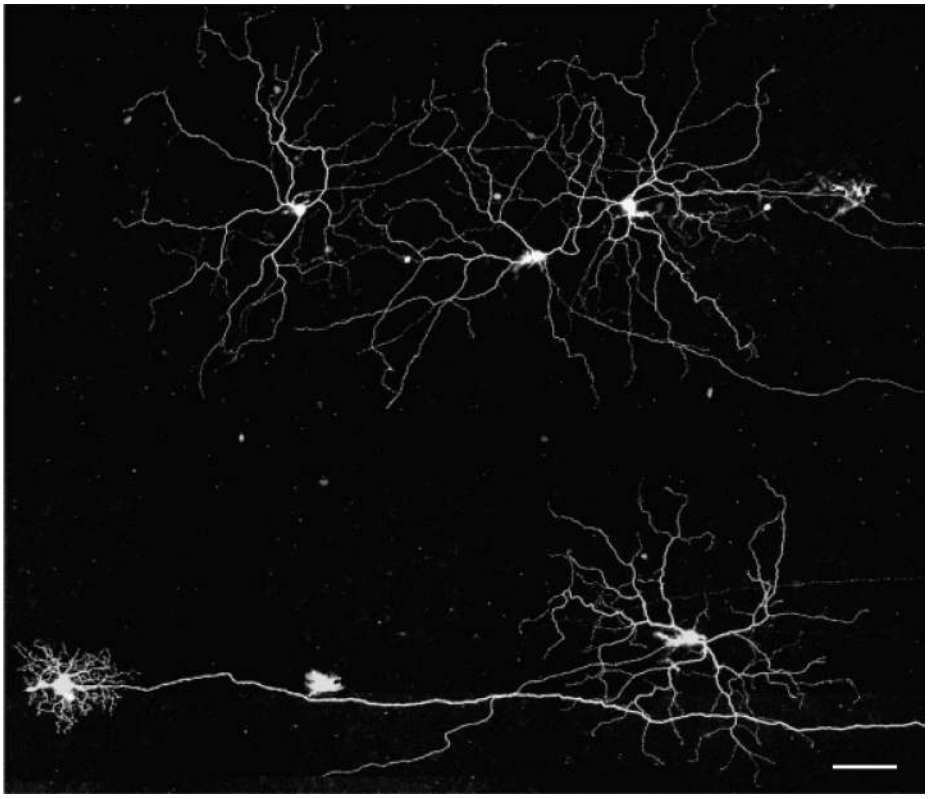

Fig. 6.

These wide-field ganglion cells were classified as large bistratified because they had complete dendritic trees in S5 and some branches arising there and ramifying in S2. They are good candidates to receive inputs from blue cone bipolar axons. They also show heterologous coupling to wide-field amacrine cells. A parasol cell (lower left) is included for comparison. Scale bar = 100 μm.

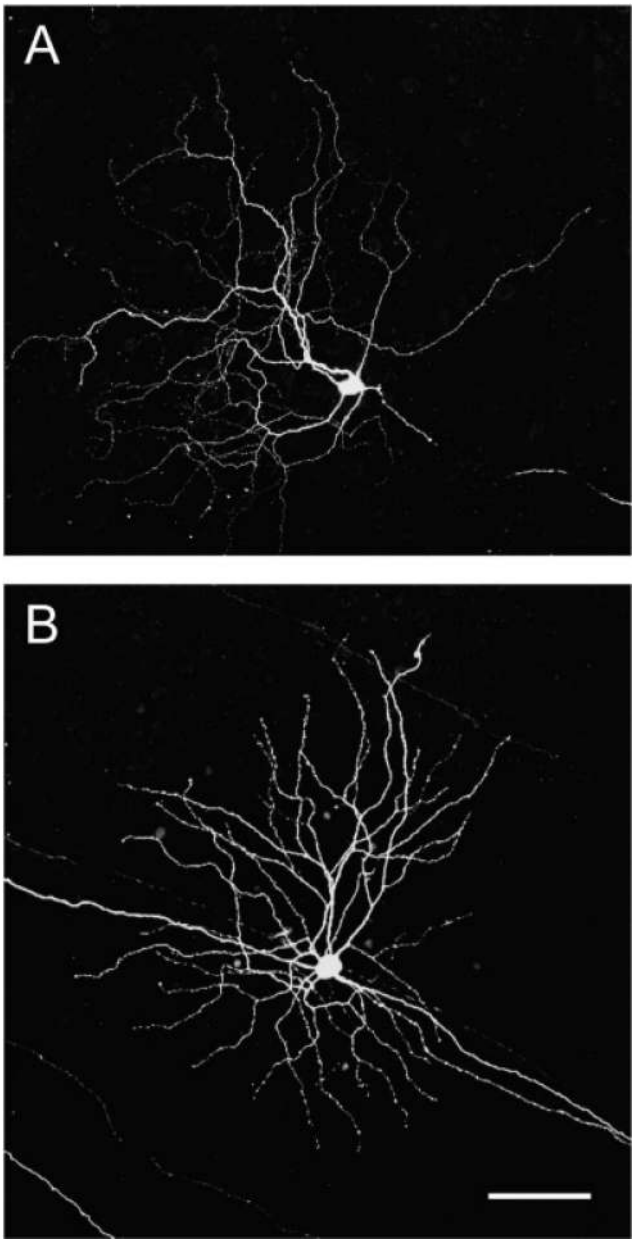

Fig. 7.

Two of the injected wide-field ganglion cells were classified as diffuse because their dendrites branched throughout the IPL. A: Diffuse thorny 11.4 mm nasal. B: Smooth diffuse 7 mm nasal. Scale bar = 100 μm.

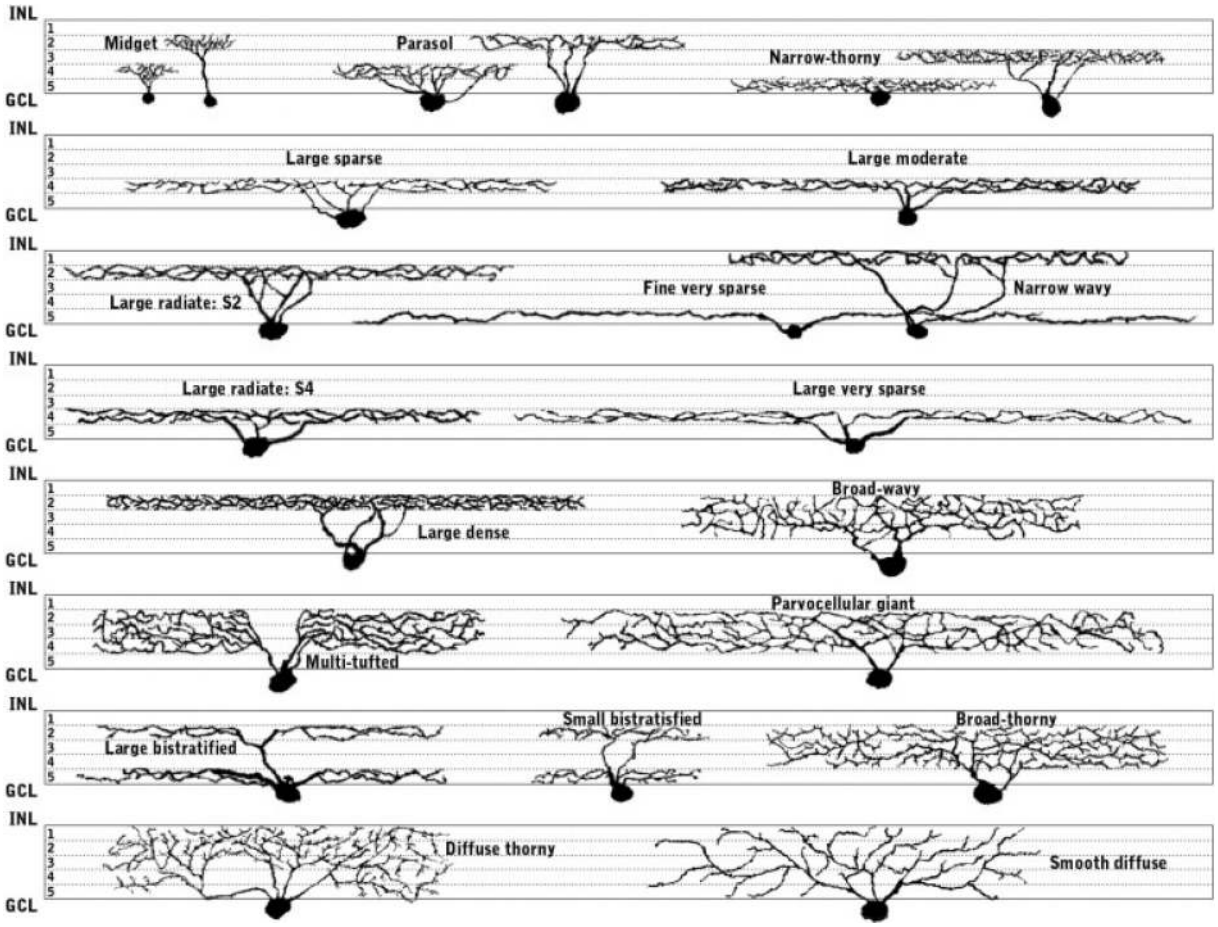

Fig. 8.

An artist's conception of the ganglion cell types described to date in macaque retinas, as they would appear in vertical sections. The five strata of the inner plexiform layer (IPL) are indicated by shading, S1 being closest to the inner nuclear layer (INL) and S5 being closest to the ganglion cell layer (GCL).

Table 1

Wide-field ganglion cells in primate retinas

This study	Kolb et al.	Rodieck & Watanabe	Dacey et al. Peterson and Dacey	Central projection	Light response
Narrow thorny	G8, G16		Narrow thorny	LGN[b]	Local edge detector[d]
Large sparse	G20		Large sparse	LGN[b]	
Large moderate	G21		Large moderate		ON direction selective[e]
Large dense		Maze	Large dense	Superior colliculus[c]	
Large radiate			Large sparse	LGN[c]	Nonlinear ON or OFF[f]
Narrow wavy	G19				
Large very sparse	G20	PT sparse	Large very sparse	Pretectum[c]	Sustained ON[g]
Fine very sparse	G3	Gamma	Giant very sparse	Pretectum[c]	
Broad thorny	G5	T group	Broad thorny	LGN[c], superior colliculus[b]	Phasic ON–OFF[g]
Multi-tufted		PT dense	Broad thorny	Pretectum[b]	ON–OFF direction selective[h]
Broad wavy		S group	Bistratified	Superior colliculus[b]	
Parvocellular giant	G23	Parvocellular giant	Large moderate	LGN[b]	Blue ON-yellow OFF[b]
Large bistratified	G17		Large bistratified	LGN[c]	
Diffuse thorny	G5		Dense diffuse		
Diffuse smooth	G22				

[a]The first column lists the 15 types of wide-field ganglion cells described in this study. The top 8 have branches restricted to only 1 of the 5 strata in the inner plexiform layer, and the second 4 branch throughout the middle 3 strata. The large bistratified cell branches in 2 distinct strata, and the last 2 types have branches throughout the inner plexiform layer. The second column lists the proposed homologues from a study of human retina by Kolb et al. (1992), and the third column gives the names used by Rodieck and Watanabe (1993) for wide-field ganglion cells in macaques. The names used by Dacey's group that were the starting point for this study are listed in column 4 (Peterson & Dacey, 1999, 2000; Dacey et al., 2003). The predicted light responses in column 5 are based on results from other species, for the most part; only the large bistratified cells have been studied using intracellular recording in macaques.

[b]Dacey et al., 2003.

[c]Rodieck & Watanabe, 1993.

[d]Amthor et al., 1989.

[e]He & Masland, 1998.

[f] Kaplan & Shapley, 1982.

[g] Isayama et al., 2000.

[h] Pu et al., 1994.